Nonstationary stochastic resonance

Redouane Fakir
Peter Wall Institute for Advanced Studies, Cosmology Group, Department of Physics and Astronomy and Department of Interdisciplinary Studies, University of British Columbia, 6224 Agriculture Road, Vancouver, British Columbia, Canada V6T 1Z1
(Received 7 January 1998)

It is by now established that, remarkably, the addition of noise to a nonlinear system may sometimes facilitate, rather than hamper, the detection of weak signals. This phenomenon, usually referred to as stochastic resonance, was originally associated with strictly periodic signals, but it was eventually shown to occur for stationary aperiodic signals as well. However, in several situations of practical interest, the signal can be markedly nonstationary. We demonstrate that the phenomenon of stochastic resonance extends to nonstationary signals as well, and thus could be relevant to a wider class of biological and electronic applications. Building on both nondynamic and aperiodic stochastic resonance, our scheme is based on a multilevel trigger mechanism, which could be realized as a parallel network of differentiated threshold sensors. We find that optimal detection is reached for a number of thresholds of order 10 and that little is gained by going much beyond that number. We raise the question of whether this is related to the fact that evolution has favored some fixed numbers of precisely this order of magnitude in certain aspects of sensory perception.
[S1063-651X(98)09806-7]

PACS number(s): 87.22.Jb, 05.40.+j

Random fluctuations are ubiquitous in physical systems, be it electronic circuits, sensory neuron networks, or any number of a large set of situations of great physical interest. This is what made the discovery of stochastic resonance [1–3] potentially a milestone in the field of signal detection. Since the early 1980s, an increasing number of authors have identified or suspected the occurrence of stochastic resonance in a wide variety of contexts [4], from paleoclimatology [1,5] to biological sensory systems [6–8] to nonlinear electronic circuits [9,10].

In the course of research on how a newly identified effect of galactic gravitational waves [11] could be detected, it was pointed out that stochastic resonance could be relevant in that context [12], since the effect in question involved (electromagnetic) *noise* in a fundamental way. It was subsequently found that applying two simple numerical threshold triggers to the data could allow the extraction of the gravitational signal from the noise [13]. In fact, this was but a specific realization of more general work on stochastic resonance than recently published [14–16]. A particularly interesting finding had just been made that systems as simple as a nondynamic trigger mechanism could display all the desirable features of stochastic resonance. The implication was that stochastic resonance, although depending crucially on the nonlinearity of the dynamics involved, may not necessarily depend on the *details* of that nonlinearity. Thus, stochastic resonance could be a more widespread phenomenon than previously thought.

More recently still, stochastic resonance was demonstrated for aperiodic signals [17–24]. More specifically, it was shown that stochastic resonance can arise for a signal that is a weak arbitrary fluctuation around some constant value, in other words, a weak stationary signal. This was an important first step towards showing that stochastic resonance is actually relevant to real-life signals, which rarely come in exact sine waves.

Here, we attempt to push these findings further by showing that, through stochastic resonance, very simple (biological or artificial) devices can also detect subthreshold signals that are not stationary. Many realistic situations call for the detection of signals of just such a nature. In fact, it is not always easy in nonlinear electronic circuits to stabilize a signal enough that it can be considered as rigorously stationary, while in biological applications the signal that is sought is seldom truly stationary. We are essentially interested in the case where the aperiodic signals already considered in the literature [17–24] have an additional nonstationary structure, i.e., a nontrivial overall time profile. It is this low-frequency aspect that we focus on, and we do not attempt to reproduce the known properties of (higher-frequency) aperiodic stochastic resonance.

Our detector is a multilevel trigger system. This could be realized, for example, as a number N of single threshold sensors mounted in parallel. Stochastic resonance in such cooperative systems has been shown to exhibit very attractive features [20,25,26], such as not requiring a finely tuned amount of noise to accomplish the detection [20]. Our system here is the equivalent of a network of parallel *differentiated* sensors: We consider a trigger mechanism characterized by a number N of thresholds of different heights. As was noted in the literature [20], such a threshold differentiation can do little to improve the detection of *stationary* signals. We now show that such multilevel trigger systems can improve the detection of signals that are markedly nonstationary. We first sketch an analytical account of roughly how one expects the system to behave, and then present the results of the actual numerical simulation in Figs. 1–4. We have consigned part of the discussion of the simulations to the captions of these figures.

Consider first the usual *single*-threshold trigger system [14–16]. Each time the input exceeds the threshold value B_1, the system generates a pulse of height H and width W. The

response is thus a pulse train $P(t)$, where t indicates the time. If the input is Gaussian white noise with rms σ and high-frequency cutoff f_0, then the response averages to

$$\langle P\rangle = HW\frac{f_0}{\sqrt{3}}\exp(-B_1^2/2\sigma^2). \tag{1}$$

Now, a subthreshold signal $S(t)$, varying on time scales much larger than $1/f_0$, is added to the input. The rate of threshold crossing will now vary in time, and the resulting response $R(t)$ can be approximated by the smeared response $\tilde{R}(t)$ (average response over time intervals that are longer than the noise correlation time and shorter than the signal's characteristic time) can be approximated by [16]

$$\tilde{R}(t) = HW\frac{f_0}{\sqrt{3}}\exp\{-[B_1 - S(t)]^2/2\sigma^2\}. \tag{2}$$

Moreover, in realistic situations (especially in biological ones), there is an upper limit to the *effective* pulse firing rate: A neuron, for example, can potentially fire a maximum of about 500 times per second. (Note, however, that as far as its interaction with the external environment is concerned, the neuron generally has the equivalent of a moving window of about 0.1 sec, so that it can react to changes in the external stimulus only at an effective rate of 10 times a second. Hence, the correct way to model the problem is highly case dependent. We are mostly interested here in the detection of a signal that is buried in *external noise*, i.e., in situations where the stimulus itself is noisy. This is the situation that arises when trying to identify the presence of a deterministic signature within a stochastic input. One must thus distinguish between internal and external noise in a more realistic model.)

There is then an effective upper limit on the rate at which the system can respond to the input, which we model by allowing each trigger to fire a maximum of about 1000 times during its exposure to a 1-sec-long signal. When the input starts crossing that trigger's threshold at a rate faster than 1000 Hz, the threshold starts firing at its maximal rate, contributing a constant value to the total output. The firing rate's upper limit is typically much smaller than the frequency cutoff f_0 of the noise. Multiplying that limit by HW, one obtains an upper ceiling R_{upper} on the value of the response function. This sudden flattening of $R_r(t)$, the more realistic response function, can be modeled algebraically in different ways, depending on the internal dynamics of the particular system considered. However, the effect of this plateau in $R_r(t)$ that we are interested in here can be captured by the following simple model:

$$R_r(t) = \min\{R_{\text{upper}}, R(t)\}. \tag{3}$$

We want to study the correlation of this output function $R_r(t)$ with the injected signal $S(t)$, which should determine whether the latter can be detected by the trigger system. We follow the literature [17,18] in using the zero-lag correlation coefficient, with the modification that our signal does not average to zero [Fig. 1(a)]. In our numerical simulations (Figs. 1–4), we of course correlate directly with the raw (pulsewise) response $R_r(t)$, not with its smeared version $R_r(t)$. But the smearing approximation is sufficient for capturing analytically the main new features brought about by nonstationarity. Note also that in several applications, especially in biological ones, it is often the gross time profiles of the nonstationary signal and of the response that are relevant, i.e., their smeared versions. Thus, we define

$$C = \frac{\langle[R_r(t) - \langle R_r(t)\rangle][S(t) - \langle S(t)\rangle]\rangle}{\langle[R_r(t) - \langle R_r(t)\rangle]^2\rangle^{1/2}\langle[S(t) - \langle S(t)\rangle]^2\rangle^{1/2}}, \tag{4}$$

and, to gain some insight into the behavior of this correlation coefficient, we briefly consider the behavior of its ''smeared'' counterpart

$$\tilde{C} = \frac{\langle[\tilde{R}_r(t) - \langle\tilde{R}_r(t)\rangle][S(t) - \langle S(t)\rangle]\rangle}{\langle[\tilde{R}_r(t) - \langle\tilde{R}_r(t)\rangle]^2\rangle^{1/2}\langle[S(t) - \langle S(t)\rangle]^2\rangle^{1/2}}. \tag{5}$$

If the total integration time is Δt, we shall compare the slope of the time profiles against the factor (see Fig. 1)

$$a \equiv \frac{B_1}{\Delta t}, \tag{6}$$

which is the slope of the diagonal across the area underneath the threshold B_1 in Figs. 1(a) and 1(b). For example, a roughly linear signal, which, when smeared, has a slope x that is much smaller than a, can be considered as virtually stationary. In that particular case, by injecting the right amount of noise to the system, it is possible to make the total input (signal plus noise) hover just about the threshold for the duration of the integration. The time features of the threshold-crossing rate will then partially reflect those of the signal, and the latter could be detected along the lines of (stationary) aperiodic stochastic resonance [17–24].

A rather different situation arises if the slope x is of the order of a, i.e., if the signal is markedly nonstationary. Consider then the simplest nonstationary case, that of a signal the smeared value of which grows almost linearly with time, e.g., $S(t) = xt + y$, where x and y are quasiconstants. If we also want the signal to start from $S(t=0) = 0$ and still remain subthreshold at the end of integration time ($t = \Delta t$), we can choose $y = 0$ and we need x to be somewhat smaller than (though still of the same order as) the nonstationarity factor a. Note finally that a more general nonstationary time profile could be qualitatively well approximated by a succession of linear sections such as the one above.

If some noise is now added to this signal, say, with an rms $\sigma \sim B_1/3$, then the total input is first well below the threshold B_1 and then well above it, with, somewhere in between, a brief critical time when the total input is just about the threshold, as in the stationary case. The output is hence first essentially zero. Then it quickly grows, over the critical time, and reaches a saturation value where it stabilizes for the remainder of the integration. [See Fig. 2(a).] This saturation can be roughly traced analytically in the behavior of Eqs. (2) and (3), upon substituting for $S(t)$ the linear form xt: If we define the normalized time

$$\tau \equiv t/\Delta t, \tag{7}$$

which grows from 0 to 1 over the integration time, we find

$$R_r(\tau)=\min\left(R_{\text{upper}},HW\frac{f_0}{\sqrt{3}}\times\exp\left\{\frac{-B_1^2}{2\sigma^2}\left[1-\frac{x^2}{a^2}\tau\left(2\frac{a}{x}-\tau\right)\right]\right\}\right). \quad (8)$$

Because the signal is below the threshold, we have $\tau<a/x$ in Eq. (7). On the other hand, we are considering the strong nonstationary case, and so $a/x\sim 1$. In addition, we have, by definition, $0<\tau<1$. Equation (7) then implies the following behavior of the system, which is confirmed by direct numerical simulation in Fig. 2. Consider first the case where R_{upper} is arbitrarily high. Then Eq. (7) implies that $R_r(\tau)$ grows almost linearly until it approaches its maximum ($\sim HWf_0$) at $\tau=1$, and hence the correlation with the input signal is quite high. This has the implication that the single-threshold systems used so far in (stationary) aperiodic stochastic resonance [17–24] have also the potential to detect nonstationary signals under certain circumstances, namely, when the pulse firing rate can be extremely fast [28].

However, in the more generic case where $R_{\text{upper}}\ll HWf_0$, the realistic response $R_r(\tau)$ is not so well correlated to the signal, as it is a function that flattens quickly when the total input crosses above the threshold. This is where multiple, differentiated thresholds can substantially improve the detection. Let us then mount, in parallel with the first, some additional trigger systems, all identical to the first except for their progressively higher thresholds (Fig. 1): $B_1<B_2<\cdots<B_N$.

The second threshold will then saturate at a higher value of τ and its output, when added to the output from the first threshold, will resemble a two-step function. With the N thresholds in parallel, one obtains an N-step total response function $R_r(\tau)$. As N increases from order 1 to order 10, the $R_r(\tau)$ profile rapidly approaches a roughly linear shape, and one expects the correlation coefficient of Eq. (4) to improve notably. However, a further increase in N towards very large values can be expected to bring about only a marginal improvement in the correlation, and this is in fact what is found numerically (Figs. 2 and 3).

As a short preview of our numerical simulations, we first note that we used a signal that increases almost monotonically with time (Fig. 1). Again, more arbitrary nonstationary profiles can often be divided into such quasimonotonic sections. Also, we purposely did not add higher-frequency structure to the signal because (1) we wanted to isolate the features brought about by nonstationarity, (2) stochastic resonance has already been successfully demonstrated for (stationary) aperiodic high-frequency signals [17–24], and (3) the signal that a system (especially a biological one) attempts to detect in the nonstationary case is often a rough time profile, and higher-frequency components are then of little relevance.

In nonstationary situations where both the overall time profile *and* the higher-frequency details of the signal are important, one can first try to detect that rough (low-frequency) time profile as described here, and then filter out the low frequencies and treat the residual signal (a *stationary* high-frequency signal) with aperiodic stochastic resonance techniques [17–24].

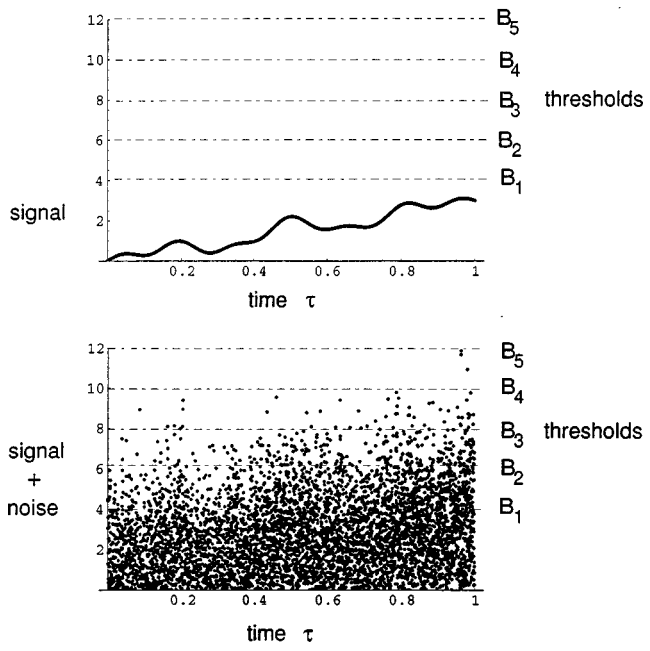

FIG. 1. (a) The N-level trigger system (here $N=5$) consists of a barrier B_1 and $N-1$ higher thresholds equally spaced between B_1 and a highest threshold B_N, chosen here to be three times B_1. (b) The deterministic input of (a) is replaced by a random looking input, obtained by adding a large amount of noise to the previous subthreshold signal.

Finally, as might be expected from previous nondynamical [14–16] and aperiodic [17–24] stochastic resonance studies, our differentiated multithreshold system, injected with nonstationary aperiodic signals, clearly displays stochastic resonance as well (Fig. 4), although it is its potential for the *detection* of subthreshold signals that is of prime importance to us here.

Describing now the simulations in more detail, we turn first to Fig. 1(a), which shows the N-level trigger system (here $N=5$) consisting of a barrier B_1 and $N-1$ higher thresholds equally spaced between B_1 and a highest threshold B_N, chosen here to be 3 times B_1. Other ways of distributing the differentiated thresholds are of course possible, but most do not lead to qualitatively different results. The signal is clearly nonstationary, and yet it remains subthreshold, i.e., undetectable in principle, throughout the integration. (The time has been normalized so that the integration runs from $\tau=0$ to $\tau=1$.)

In Fig. 1(b), the deterministic input of Fig. 1(a) is replaced by a random looking input, obtained by adding a large amount of noise to the previous subthreshold signal. The noise here is a low-pass filtered, zero-mean Gaussian white noise. The input now clearly exceeds the barrier B_1 and a few more thresholds. When any of the thresholds is exceeded, the system fires a pulse of standard (but otherwise arbitrary) height H and (narrow) width W. At any given time τ, the response $R(\tau)$ is the sum of the outputs from all the thresholds exceeded at that time τ. I.e., if B_j is the highest threshold exceeded at τ, then $R(\tau)$ is a pulse of width W and height $j\times H$.

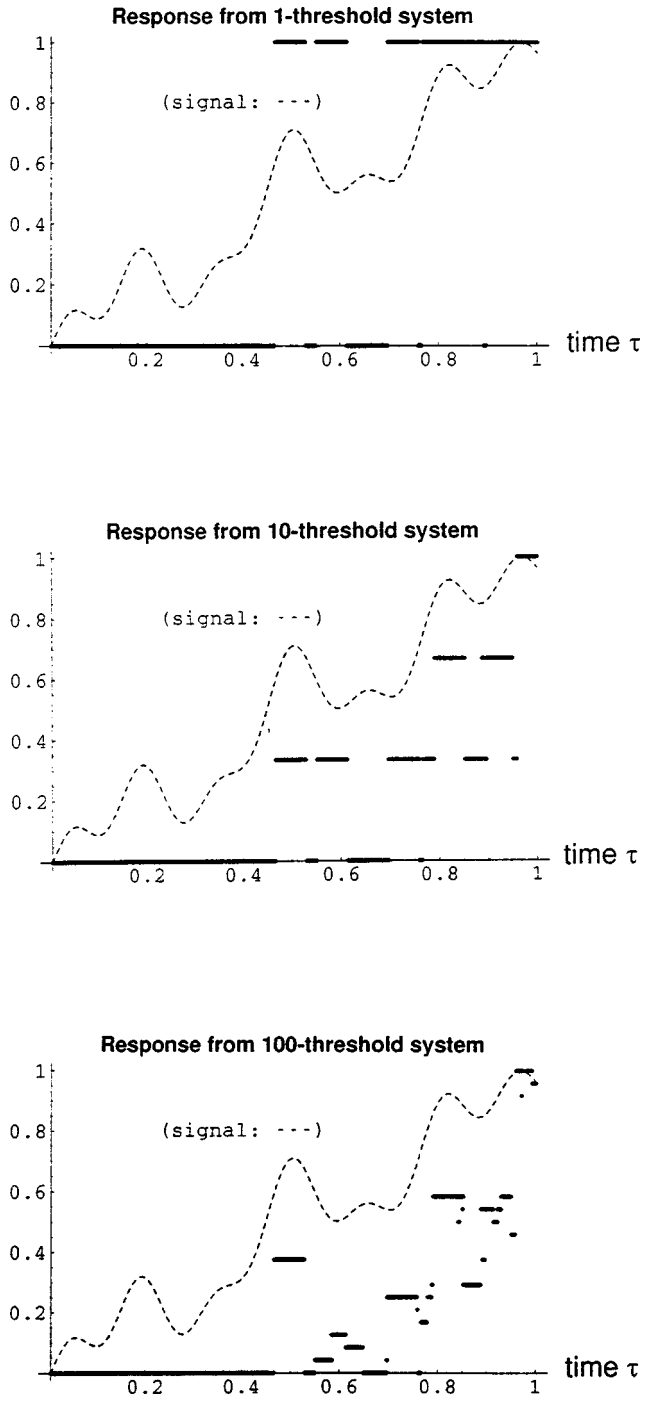

FIG. 2. (a) The subthreshold input signal of Fig. 1(a) and the response $R(\tau)$ of the trigger system, both rescaled here and in (b) and (c) below, for easier visual comparison. When only one threshold (that is, B_1) is activated, the response is roughly a step function. (b) When N, the number of thresholds, is greater than 1 (here $N=10$), the response takes the aspect of a multistep function [again rescaled here as in (a)] that follows roughly the nonstationary profile of the signal. (c) When the number of thresholds becomes large (here, $N=100$), the steps and the stochastic broken lines become comparable in length, resulting in a scattered response function.

Figure 2(a) shows the subthreshold input signal (thin dashed curve) of Fig. 1(a) and the response $R(\tau)$ of the trigger system. [Both are rescaled here and in Figs. 2(b) and 2(c), for easier visual comparison.] When only one threshold (that is, B_1) is activated, the response is roughly a step function: For small values of τ, most of the points in Fig. 1(b) are below B_1 and hence produce a zero response, while for large values of τ, most of the points are above B_1 and produce a response equal to $1\times HW$ (scaled here to 1.) One can see that this one-step response function is only marginally correlated to the underlying signal, which translates into a low value of the correlation coefficient for $N=1$ in Fig. 3.

From Fig. 2(b) one can see that when N, the number of thresholds, is greater than 1 [$N=10$ in Fig. 2(b)], and each of the exceeded thresholds (here, there are four) contributes a different step function to the response. Hence, the latter takes the aspect of a multistep function [again rescaled here as in Fig. 2(a)] that follows roughly the nonstationary profile of the signal. There is a clear improvement of the correlation between the response and the signal, confirming our earlier heuristic argument which used the smeared approximation $\tilde{R}(\tau)$ to the response $R(\tau)$.

Because the quasistep functions due to the individual thresholds are partially stochastic, they also contribute some broken lines to the total response, as can be seen in Figs. 2(a) and 2(b). When, as in Fig. 2(c), the number of thresholds becomes large [$N=100$ in Fig. 2(c)], the (now very short) steps and the stochastic broken lines become comparable in length, resulting in a scattered response function. As a consequence, the correlation between signal and response is not much stronger than in the case $N\sim 10$, and hence the leveling off of the correlation coefficient as a function of N in Fig. 3.

Figure 3(a) shows the correlation coefficient of Eq. (2), which is the value of the normalized correlation function (between the response and the signal) at zero lag. The increase of the correlation with the number of thresholds levels off at $N\sim 10$, as was foreseen in the above discussion of Fig. 2. (The first three values of N produce the same correlation because, for these small values, the space between thresholds is large enough that only B_1 is exceeded.) Thus, a number of order of magnitude 10 of differentiated, individual triggers, mounted in parallel (summed outputs), is singled out for the optimal detection of a nonstationary signal.

Figure 3(b) confirms that the main feature of Fig. 3(a), i.e., the plateau of the correlation coefficient as a function of the number N of thresholds, is robust in the large-N limit. In both Figs. 3(a) and 3(b), the calculations were performed using a noise with rms σ equal to half the height of the first barrier B_1.

Finally, Fig. 4 shows the correlation coefficient C of Eq. (4) as a function of σ, the rms of the noise, divided by the lowest threshold B_1. The system clearly displays stochastic resonance. When there is more than one threshold ($N>1$), the decrease of C becomes slightly sharper when σ exceeds a value of order 1. This is a consequence of having a fixed highest threshold, namely, $B_1+2\times B_1$ (see Fig. 1): When the noise is large enough that its tip starts exceeding the highest threshold (which occurs when $\sigma\sim B_1$), the whole system starts behaving more like a one-threshold system and hence the sharper decrease in C (compare with the $N=1$ curve.) Note that for N of order 10 or larger, all curves are nearly identical to the $N=1000$ curve shown in Fig. 4. So, although there is a clear broadening of the stochastic resonance curves

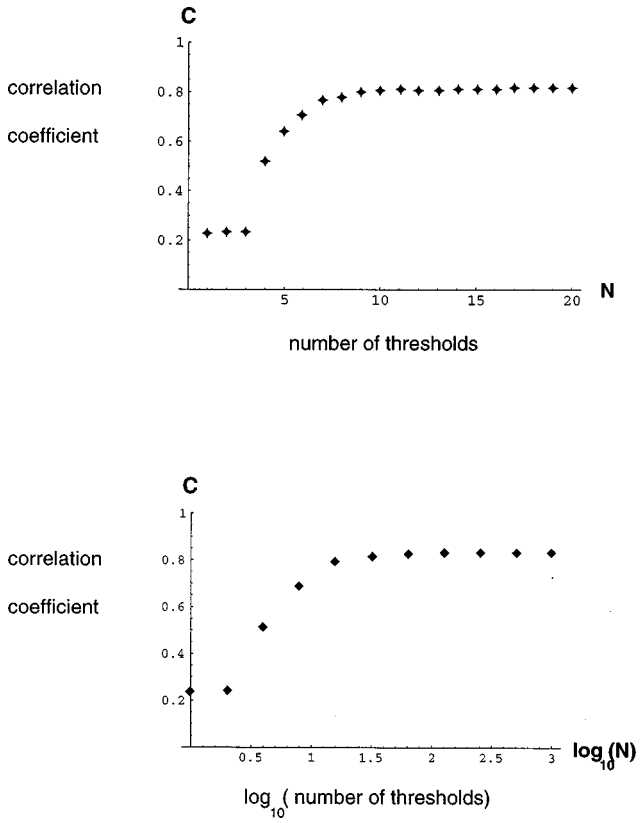

FIG. 3. (a) The correlation coefficient of Eq. (2), which is the value of the normalized correlation function (between the response and the signal) at zero lag. The increase of the correlation with the number of thresholds levels off at $N \sim 10$, as was foreseen in the text. Thus, a number of order of magnitude 10 of differentiated, individual triggers, mounted in parallel is singled out for the optimal detection of a nonstationary signal. (b) The result of (a) above; i.e., the plateau of the correlation coefficient as a function of the number N of thresholds, is robust in the large-N limit.

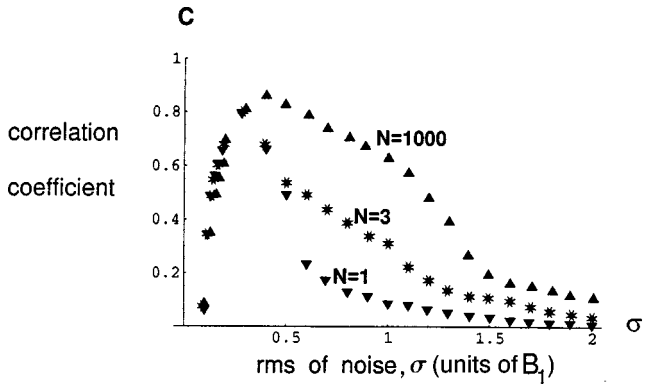

FIG. 4. The correlation coefficient C of Eq. (4) as a function of σ, the rms of the noise, in units of the lowest threshold B_1. The system clearly displays stochastic resonance. (See the text for more on these specific profiles.)

(and hence less fine-tuning of the noise is necessary to detect the weak signal) for large values of N, this system is not as free of fine-tuning as the (nondifferentiated) multithreshold system described in the (stationary) aperiodic stochastic resonance literature [20,25,26] referred to earlier in the text.

In all, our study suggests that stochastic resonance might be exploited for the detection of even strongly nonstationary subthreshold signals. We find that a differentiated multiple-threshold system might, in such cases, improve on the performance of single-threshold systems. But this is by no means a universal conclusion: we find numerically the amount of improvement to be strongly case dependent (i.e., depending on the shape of the signal, the noise characteristics, etc.). The results reported here are for cases where the multithreshold scheme presents a clear advantage. A thorough investigation of the comparative performance of differentiated multithreshold systems throughout parameter space is underway [27]. Also, the capacity of *modified* single-threshold systems to detect realistic nonstationary signals has also been investigated recently [28].

One example of a differentiated multiple-threshold system that might function similarly to our theoretical system is the auditory sensory system in mammals. In this system, each primary afferent neuron (from the spiral ganglion) has its lowest threshold to a particular frequency of sound, called its ''characteristic frequency.'' Its threshold is increasingly higher for sound frequencies farther from the characteristic frequency. When the system is stimulated by a weak pure tone of a given frequency, only neurons with a characteristic frequency near the stimulating frequency, and thus having low thresholds for those sounds, will fire. As the tone increases in amplitude, the first-firing neurons will quickly saturate but other neurons, whose thresholds for the stimulating frequency are higher because their characteristic frequencies are farther from it, will begin to fire as their thresholds are exceeded. In this way, the number of neurons firing will track the intensity of the pure tone. If these neurons converged upon an integrator neuron whose firing depended directly on the firing of several spiral ganglion neurons with different characteristic frequencies, the integrator would fire proportionately to the signal amplitude. This system would give a similar response for a subthreshold signal that was amplified above the thresholds of the auditory receptors by environmental or internal noise, i.e., in the stochastic resonance situation. Such circuits in the auditory system have been argued to be responsible for the primary coding of auditory signal intensity [29] and for the integration of intensity information from very brief auditory signals [30].

Our simulations suggested that only a relatively small number of cooperative trigger mechanisms (of order 10 in our study) might be necessary to achieve near-optimal detection of subthreshold signals, at least nonstationary ones. This result is reminiscent of the fact that some key components of certain biological systems consist of a fixed number of receptors mounted in cooperative neural networks similar to our differentiated multithreshold system. For example, under optimal conditions a minimum of six photons must each stimulate a different rod in the retina of the eye, the signals from the six rods being integrated in the response of a single retinal ganglion cell [31]. This is not a stochastic resonance situation, since the rods are roughly identical near-ideal detectors responding to single photons, and Poisson noise from the source only degrades that function. However, it is interesting that evolution has developed such a sparse network that can be so exquisitely sensitive to environmental signals.

Perhaps there is a more general principle of diminishing returns operating that keeps such cooperative networks small even though they are of diverse function. We speculate that this principle might be important in the functioning of stochastic resonance in some biological systems and that evolution may have exploited it to enhance the detection of a wide class of fitness-relevant environmental signals, in particular nonstationary signals as described here.

Clearly, however, much more detailed studies of biologically (or electronically) plausible multiple-component, stochastic resonance systems, injected with a variety of realistic signals, must be conducted before such an evolutionary role of stochastic resonance is confirmed.

I am grateful to to L.M. Ward for much information about neural processes and to P.E. Greenwood for reviewing the paper and making several suggestions. I am indebted to W.G. Unruh for bringing the phenomenon of stochastic resonance to my attention and to B. Bergersen for providing previous literature on the topic. I am grateful for the extensive logistical support.

[1] R. Benzi, S. Sutera, and A. Vulpiani, J. Phys. A **14**, L453 (1981).
[2] C. Nicolis, Tellus **34**, 1 (1982).
[3] R. Benzi, G. Parisi, A. Sutera, and A. Vulpiani, Tellus **34**, 10 (1982).
[4] K. Wiesenfeld and F. Moss, Nature (London) **373**, 33 (1995).
[5] C. Nicolis, J. Stat. Phys. **70**, 3 (1993).
[6] A. Longtin, A. Bulsara, and F. Moss, Phys. Rev. Lett. **67**, 656 (1991).
[7] J.K. Douglass, L. Wilkens, E. Pantazelou, and F. Moss, Nature (London) **365**, 337 (1993).
[8] S.M. Bezroukov and I. Vodyanoy, Nature (London) **378**, 362 (1995).
[9] S. Fauve and F. Heslot, Phys. Lett. **97A**, 5 (1983).
[10] R.N. Mantegna and B. Spagnolo, Phys. Rev. E **49**, R1792 (1994).
[11] R. Fakir, Int. J. Mod. Phys. D **6**, 49 (1997); Phys. Rev. D **50**, 3795 (1994); Astrophys. J. **426**, 74 (1994).
[12] W.G. Unruh (private communication).
[13] R. Fakir (unpublished).
[14] P. Jung, Phys. Rev. E **50**, 2513 (1994); Phys. Lett. A **207**, 93 (1995).
[15] K. Wiesenfeld, D. Pierson, E. Pantazelou, C. Dames, and F. Moss, Phys. Rev. Lett. **72**, 2125 (1994).
[16] Z. Gingl, L.B. Kiss, and F. Moss, Europhys. Lett. **29**, 191 (1995).
[17] J.J. Collins, C.C. Chow, and T.T. Imhoff, Phys. Rev. E **52**, R3321 (1995).
[18] J.J. Collins, C.C. Chow, A.C. Capela, and T.T. Imhoff, Phys. Rev. E **54**, 5575 (1996).
[19] J.J. Collins, T.T. Imhoff, and P. Grigg, J. Neurophysiol. **76**, 642 (1996).
[20] J.J. Collins, C.C. Chow, and T.T. Imhoff, Nature (London) **376**, 236 (1995).
[21] J.E. Levin and J.P. Miller, Nature (London) **380**, 165 (1996).
[22] C. Heneghan, C.C. Chow, J.J. Collins, T.T. Imhoff, S.B. Lowen, and M.C. Teich, Phys. Rev. E **54**, R2228 (1996).
[23] P.C. Gailey, A. Neiman, J.J. Collins, and F. Moss, Phys. Rev. Lett. **79**, 4701 (1997).
[24] A. Neiman, L. Schimansky-Geier, and F. Moss, Phys. Rev. E **56**, 9 (1997).
[25] E. Pantazelou, F. Moss, and D. Chialvo, in *Noise in Physical Systems and 1/f Fluctuations*, edited by P.H. Handel, AIP Conf. Proc. No. 285 (AIP, New York, 1993), pp. 549–552.
[26] F. Moss and X. Pei, Nature (London) **376**, 221 (1995).
[27] L. Ward, P. Greenwood, and R. Fakir (unpublished).
[28] R. Fakir (unpublished).
[29] R.D. Luce and D.M. Green, Psychol. Rev. **79**, 14 (1972).
[30] L.M. Ward, Percept. Psychophys. **50**, 117 (1991).
[31] S. Hecht, S. Schlaer, and M.H. Pirenne, J. Gen. Physiol. **25**, 819 (1942).